DEVELOPMENT OF HIGH-PERFORMING NOVEL HETEROGENEOUS FENTON-LIKE CATALYSTS FOR THE ABATEMENT OF ORGANIC POLLUTANTS: AN OVERVIEW

ABHILASHA JAIN [a] AND CHETNA AMETA [b]*

[a]*Department of Chemistry, St. Xavier's College, Mumbai 400001, Maharashtra, India.*
[b]*Photochemistry Laboratory, Department of Chemistry, University College of Science, M. L. Sukhadia University, Udaipur 313002, Rajasthan, India.*

ABSTRACT

Fenton reagent is known for over a hundred years and the role of homogeneous and heterogeneous Fenton degradation in wastewater treatment in removing recalcitrant organic contaminants is well appreciated and extensively explored. Limitations and shortcomings of homogeneous and heterogeneous Fenton degradation hinder the large-scale application of heterogeneous Fenton reactions in environmental remediation. Thus, the development of Fenton-like reagents is considered as a need of the hour. Most of the drawbacks of Fenton degradation have been taken care of by these novel reagents were dramatically increased catalytic degradation rate of contaminants was observed due to high surface area. Good mechanical stability, improved electron transfer, magnetically separability, and the possibility of widening the scope are the additional features of Fenton-like reagents. In this review, recent trends in the synthesis, strategies for enhancing its catalytic activity, and various applications of heterogeneous Fenton-like catalysts for the abatement of organic pollutants are discussed. This review describes the recent development of other transition metals, Graphene oxide/Carbon/CNT, MIL/MOF, and oxides as Fenton like catalysts in environmental remediation procedures even at ambient conditions. This review aims to encourage the fabrications of novel and efficient heterogeneous Fenton-like systems and assist the readers in the selection of the best suitable Fenton-like systems for industrial applications by unfolding the various properties and applications of these catalysts.

Keywords: Fenton like reagents, Graphene oxide/Carbon/CNT, MIL/MOF, SiO_2 and TiO_2, degradation of organic pollutants.

1. INTRODUCTION

Currently, treatment of extremely toxic organics in polluted water fascinates more attention since they are dangerous to the surroundings. Through the last spans, Fenton's process has been deliberate in direction to improve its proficiency in the depuration of liquid sewage [1,2]. Advanced Oxidation Process (AOP) can eliminate and reacts to the organic material by producing the vigorous oxidant hydroxyl via the breakdown of hydrogen peroxide in the exi stence of iron ions at acidic medium. Furthermore, the catalytic decay of hydrogen peroxide exhibits a radical mechanism comprising hydroperoxyl radicals. Oxidation is originated by the hydroxyl radicals that will react non-selectively on organic material present in the effluents. The foremost advantage of this process is linked with the context that the reaction completed at room surroundings of temperature and pressure which creates the process low-cost. Fenton's procedure has a significant role either to endorse the wastewater management to achieve the boundaries standard to an innocuous discharge into the water passages or to diminish the effluent harmfulness and improve its biodegradability to permit an effective post-biological depuration in civic wastewater treatment plants.

To overcome the restraint of the Fenton process and advance the pollutant degradation efficiency, light irradiation was introduced into the Fenton system to practice the photo-Fenton process. Advanced Fenton process (AFP) is executed for enhanced handling ability and superior energy productivity. Fenton reaction often utilized Fe-lush clays as heterogeneous catalysts like Tejera-Esghira clay having iron oxide units on the surface. The use of natural clay as a Fenton catalyst is an innovative and attractive substitute due to the hugely available and inexpensive catalyst with great iron content. Natural Tunisian clay/red clay (RC) was employed as a natural adsorbent/heterogeneous catalyst (photo-Fenton) for the elimination of 2-chlorophenol and Cd (II) in aqueous schemes [3]. The adsorption of Cd ions on natural RC (Tejera-Esghira) was found to be the pseudo-second-order reaction. Langmuir model helped to determine the maximum adsorption ability of acid-activated clay i.e., 23.59 mg g1. Photo-Fenton experimentations verified high activity of the natural clay, which was capable to entirely degrade the phenol in 30 min with the ultraviolet light C (UV-C).

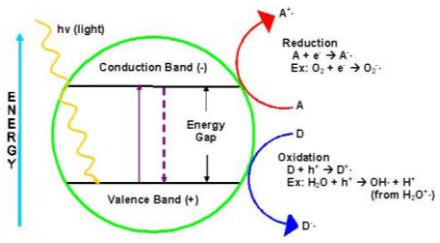

Figure 1. Principle of photocatalysis.

The occurrence of numerous organic chemicals in wastewater obtained from industrial leakage and effluent. These organic compounds are a great threat to public health since they are hazardous. So removal from the contaminated water is very essential. Fenton's oxidation can be used as an operative pre-treatment phase since they can transform pollutants into by-products that are easily decomposable and thus reduces total toxicity towards microorganisms. Fenton's oxidation method is a supreme way to proceeds with metal-catalyzed oxidation reactions of organic compounds (water-soluble). The Fenton's reagent has two functions including oxidation then coagulation. The coagulation further eliminates the residual impurities after Fenton's oxidation. The pH ranges from 2-4 since at the lower side i.e., at pH < 2.0 the reaction is decelerated because of complex formation between iron species and $[H_3O_2]^+$ (oxonium ion) as a higher range (pH > 4) the production of hydroxyl radicals gets reduced due to ferric-hydroxo complexes formation. AOPs typically work with fewer energy conditions than direct oxidation. AOPs needs ambient temperature and involve the hydroxyl radical generation in adequate quantity to affect water decontamination. Fenton's reagent has two key components first one is catalytic chemical species and a chemical oxidant. Mainly Fe^{2+}or Fe^{3+} work as catalysts and H_2O_2 as oxidizing agents in traditional Fenton's reaction.

Ibuprofen (IBP) is an anti-inflammatory, non-steroidal painkiller which is extensively applicable for the cure of various diseases like migraine, muscle pain, and fever. It is liberated with its metabolites into nature either by industrial or domestic paths. Both metabolites and IBP are highly tenacious and have bad impacts on aquatic and terrestrial animals. A new heterogeneous Fenton-like catalyst was utilized for the mineralization of Ibuprofen, a drug frequently found in waste sludge [4].

The Fenton-reactions were executed in a batch scheme. They used copper/iron-doped zirconia samples against mineralization and degradation of IBP. The finest catalyst was copper held over zirconia, which accomplished a practically complete decay of IBP (98 %) and 50 % of mineralization. Process productivity was enhanced by optimizing the critical parameters such as pH, oxidant dose, temperature, and catalyst loading. Furthermore, these catalysts do not yield toxic metabolite which is very important, when considering the water treatment.

Bulk Fe_3O_4 is ferromagnetic; Fe_3O_4 NPs are superparamagnetic, which offers a stronger magnetic reply when placed in a magnetic field. This feature drew attention towards Fe_3O_4 NPs in contrast with old-style iron-based catalysts because their magnetic behavior offers a fast, feasible, and easy way of separation from the reaction medium so that can be reused. The immobilization of ZnO/ TiO_2 NPs in Fe_3O_4 NPs offers not only easy recapture of the catalyst but also a dual-nature nanocomposite as a photo-Fenton agent. Feijoo et al. [5] displayed the prominence of identifying the significance of NPs production approach in the environmental ways connected with their implementation. They fabricated Fe_3O_4 NPs and makes nanocomposites of TiO_2 or ZnO NPs that stayed onto Fe_3O_4 NPs as Fenton agents.

**Corresponding author email: chetna.ameta@yahoo.com*

Potassium ferrite is an ecologically pleasant iron oxide that showed super-high ion conductivity and exceptional thermal constancy. Its 3D structure is made up of tetrahedral FeO_4 and octahedral FeO_6 with common edges and vertices. Thus, the structure developed is a dominant candidate for a heterogeneous photo-Fenton catalyst for the degradation of contaminants. Potassium ferrite ($K_2Fe_4O_7$) crystals have hexagon-shape with different sizes were synthesized using the hydrothermal method by Zhang et al. [6] The produced crystals displayed a bandgap of 1.44 eV and was utilized as heterogeneous Fenton catalyst to abolish methylene blue (MB) and crystal violet (CV) dye under visible-light radiation in the presence of H_2O_2 (green oxidant). Their average size was found 20 μm and show superior photocatalytic activity since it has a large surface area. When it was employed for the photo-Fenton reaction it degrades 100% MB and 92% CV within 35 min. Additionally, the catalyst was stable after four constant cycles. The trapping investigations revealed that the active hydroxyl radical (·OH) was dominant in the reaction.

Newly, magnetically detachable nanosized photocatalysts are extensively studied. Particularly Nano ferrites having a distinctive magnetic character are highly appropriate. These ferrite nanoparticles (NPs) are used in heterogeneous photocatalysis and their catalytic activity relies on the surface area, particle size, red-ox properties of metal ions, morphology, the distribution of metal ions among the lattice spots, and doping. Alkaline-earth metal ion has excellent proficiency in the photo-Fenton system due to its stability, electron-donating, and economic feasibility. Nadeem et al. [7] studied the synthesis then the characterization of $ZnFe_2O4$ and graphene oxide-based $ZnFe_2O_4$ composite and employed for synzol red reactive dye degradation. Results showed 57 and 94 % degradation by $ZnFe_2O_4$ and graphene oxide-based $ZnFe_2O_4$ respectively. Nadumane et al. [8] described an innovative green method to synthesize pure and $NiFe_2O_4$: Mg^{2+} (1 mol %) catalyst by modifying sol-gel technique and utilized in photocatalysis and LED to enhance photoluminescence nature.

Antibiotics create a new class of contaminants since their amounts are increasing rapidly in effluent and possess harmful effects on the environment. Physical adsorption and microorganism treatments are insufficient to treat antibiotics. AOP especially Fenton-based catalyst achieved high degradation against antibiotics and other drugs. Li et al. [9] prepared mesoporous bimetallic Fe/Co and employed it as a Fenton-like photocatalyst to destroy the tetracycline hydrochlorides (TC). The bimetallic catalyst was reusable and found to have great stability. The Fe/Co catalyst has outstanding catalytic efficacy with a broad pH range and contains smaller quantities of leached ions which boost its potential uses. Thus it was confirmed that the transition metals with heterogeneous catalysts not only enhance the catalytic performance but also enhances the reaction conditions by the synergistic effect of various metals present. Du et al. [10] investigated the efficiency and viability of a heterogeneous photo-Fenton catalyst, Fe/Si co-doped TiO_2 synthesized using sol-gel method, for the dilapidation of metronidazole (MNZ) antibiotics under visible light exposure. Metronidazole was degraded in less than an hour (50 min). Thus catalysts with exceptional catalytic activity and outstanding reusability and stability provide an innovative perception into the preparation and utilization for antibiotics elimination.

Nowadays, a range of synthetic pesticides is available to enhance agricultural manufacture. Imidacloprid (IMI) is one of them since has highly toxic, quite greater solubility (0.58 g L^{-1}), and permanency in water. IMI is a general chloronicotinyl pesticide and displays the acute intoxication homes for a living organism. Hence it needs of hour to degrade pesticide using the heterogeneous Fenton method. Liu et al. [11] examine the mineralization of IMI (commercial pesticide) decay by the heterogeneous photo-Fenton process. They utilized discarded iron oxide (labeled as BT) for the mineralization of pesticides in terms of TOC elimination. The results open that TOC removal proficiency increases with an increment in H_2O_2 amount till 105.0 mM, an upsurge in catalyst dosage from 1.0 to 5.0 g L^{-1}, and a drop in pH from 5.0 to 3.5. Under the ideal conditions, 97.7% TOC elimination was attained in 6 h under 254-nm UV radiation. Furthermore, recycling investigates directed that the iron oxide (waste) had decent stability and the TOC exclusion of pesticide yielded greater than 80% even after fourth recycles.

There are two types of zeolites present i.e., are synthetic and natural. Synthetic zeolites possess homogeneous configuration, sharp properties, and a definite arrangement that depends on the control of the method of preparation. These features permit their application in selective high-performance reactions and are widely applicable in commerce, but they are expensive in contrast to natural zeolites. Natural zeolites have a heterogeneous configuration, their properties and structure vary widely from one another. Even though natural zeolites are not very selective, plenty, crystalline and reactive with ion exchange capacity. They allow the adsorption of minerals like C, Ca, K, Na, Fe, and Mg and useful in numerous chemical reactions. That's why natural zeolites are a good option for the heterogeneous catalyst. Pure zeolites are photocatalytically inactive since they do not show any absorption in the UV-vis region whereas adsorption of heterogeneous atoms into zeolite lattice makes them photocatalytically active. Zeolites tend to adapt their structural nature (porosity, mechanical composition, chemical properties, and strength among other properties) via calcination procedures. Domenzain-Gonzalez et al. [12] used Mexican natural zeolite (MNZ) and increase the Fe concentration to enhance its performance via an incipient wetting method. The impregnated zeolite (MNZ/Fe) was employed for RB5 dye degradation via the heterogeneous photo-Fenton procedure and the influence of calcination temperature was studied on the catalyst. The RB5 dye degradation was accomplished in 180 min with 93 % discoloration and 70.5 % chemical oxygen demand.

Chromite is an oxide mineral $FeO.Cr_2O_3$ (68% Cr_2O_3, 32% FeO) belongs to a class of spinel group and develops in the isometric system. It is the foremost source of chromium on the earth and is used by many industries including refractory, metallurgical, and chemical industries. Shaban et al. [13] employed natural chromite for the destruction of Congo red dye via photocatalytic and photo-Fenton oxidation of wastewater. Another fascinating material is hematite (α-Fe_2O_3) since is the highly stable iron oxide having n-type semiconducting features in at room environment. Due to the attractive features like natural richness, budget, harmless, chemical steadiness with a 2.2 eV optical band gap, Fe_2O_3 is a suitable candidate for photocatalysis applications. Yang et al. [14] fabricated Fe_2O_3/MoS_2 and used it as a photocatalyst for the decay of Methyl orange (MO) contaminant and the experiment revealed 84% of the early capacitance residual after 2000 cycles. It is supposed that the usage of graphene-α-Fe_2O_3 hybrid structures can improve electron transport from the semiconductor to the graphene substrate as a charge accumulator. Frindy and Sillanpa [15] incorporated different amounts of graphene sheets into iron oxide using a green and easy hydrothermal process and used for visible light degradation of RhB (Rhodamine B) in industrial effluents. The result revealed 98 % degradation under visible light radiation.

Recently, metal-organic framework (MOF), a new class of hybrid practical materials has grabbed all attention for their topologies, compositions, and varied structures. The MOFs-template method has been approved to form metal/metal oxide micro/nanostructures with numerous precise shapes including nanowires, nanorods, microplates, nanoparticles, hollow, nanosheets, and coralloid nanostructures by precursors, controlling reaction temperature and time. Normally, MOFs are recognized for their large surface areas with greater adsorption capacity and thus have involved considerable curiosity in various applications including Fenton-like reaction. Wang et al. [16] synthesized porous carbon-coated Fe_3O_4 was synthesized based on the solid-template scheme. The hierarchical Fe_3O_4/carbon superstructures with diverse morphologies can be attained by pyrolysis of MIL-88A. In this review, we deliberated the recent growths in heterogeneous photocatalysts for photo-Fenton systems including MIL, transition metals, MOF, oxides, and carbon grounded catalyst.

2. Fenton-Like Catalysts Using transition metals: Cu, Mn, Co, Ni, Al, Cr

2.1 Copper-based catalyst

A bimetallic catalyst (CuVOx) was synthesized by a hydrothermal method which was employed for degradation of fluconazole where higher catalytic activity, wider pH range, and more recyclability of catalyst were reported. Due to the presence of vanadium the reactivity of the copper catalysts in terms of adsorption capacity, surface defects, and active site concentration were improved. It was concluded that electron-rich centers around Cu/V active sites and surface hydroxyl groups play a key role in improved catalytic activity.

A novel magnetic Cu-Fe oxide (CuFeO) was fabricated as the heterogeneous photo-Fenton catalyst in a two-step method by Cheng etet al. [17] which can be employed at slightly basic pH conditions for the removal of antibiotics namely sulfamethazine. The mechanistic details were studied using X-ray photoelectron spectrum analysis, radical scavenging, and electron spin-trapping experiments.

It was proposed that due to the synergistic effect among photo-induced electrons, Copper and iron in CuFeO exhibits brilliant performance in the catalytic activation of H_2O_2.

The effect of tartaric acid on the heterogeneous photo-Fenton-like degradation of methylene blue catalyzed by $CuFe_2O_4$ was investigated by Guo et al. [18]. The increased catalytic activity can be ascribed as more generation of hydroxyl radicals, reduction in the leaching of metal ions occupying B-sites, and inhibit the formation of iron sludge. It was suggested that Fe^{3+} and Cu^{2+} reacted with tartaric acid to form a stable homogeneous photo-Fenton-like system by LMCT pathway.

Ag_3PO_4/CuO composites were prepared by Ma et al. [19] via hydrothermal and ion exchange reactions which act as photocatalyst as well as Fenton-like CuO catalysis. The optimized composite exhibited a significant improvement in catalytic activity to decomposed organic pollutants due to the synergistic effect of photocatalysis and Fenton-like catalysis and its activity retained even after five cycling runs. The study of mechanistic details indicated the matched band structures, Z-scheme photocatalytic mechanism, and the generation of a large number of hydroxyl radicals.

Ordered mesoporous silicon supported Fe-Cu bimetallic catalyst (Fe-Cu@MPSi) was synthesized by Zheng et al. [20] which exhibited high heterogeneous Fenton-like activity for degradation of ofloxacin (OFL). The enhancement in catalyst activity has been attributed to the ordered mesoporous structure, uniform mesopore size (~2.4 nm), moderate pore volume (0.19 cm^3/g), high BET surface area, and highly dispersed Fe_2O_3 and CuO nanoparticles in the mesopore channels as well as the surface of the catalyst which owes the synergetic interfacial effect of Fe and Cu on the surface of the catalyst and the complexation of OFL and cupric ions.

An attempt has been made by Zhang et al. [21] for the fabrication of high crystalline CuO fibers by an electrospinning method and its photo Fenton-like activities have been assessed for the degradation to methyl orange. It was concluded that H_2O_2 accepted the photogenerated electrons and holes effectively which inhibited the recombination of charge carriers and it generated more hydroxyl radicals. The well-crystalline of CuO fibers also enhanced its photocatalytic activity.

Alumina-supported bimetallic Fe-Cu catalysts were prepared by the sol-gel method. It was observed that the synergism between Fe and Cu species encouraged the reduction of Fe^{3+} to Fe^{2+}, thus accelerate the generation of hydroxyl radicals (•OH) and enhanced the catalytic activity towards the degradation of nitrobenzene (NB).

Subbulekshmi and Subramanian [22] synthesized CuO/FAZ; a novel, stable, reusable heterogeneous Fenton-like catalyst by coal fly ash converted and nano CuO fringes incorporated zeolite X material (CuO/FAZ). CuO/FAZ by ion exchange with Cu^{2+}, and subsequent calcination of zeolite for the wet peroxide degradation of p-nitrophenol and p-nitroaniline.

Xie et al. [23] fabricated Fenton-like catalyst γ-Cu-Al_2O_3-$Bi_{12}O_{15}Cl_6$ for selective degradation of phenolic compound. In this catalyst due to the high electronegativity of Bi and electron-poor Cu center is formed which enables the formation of σ-Cu-ligand which gets reduced by oxidization of the HO-adduct radicals which lead to a generation of hydroxyl radical and improved the redox cycle of Cu(II)/Cu(I),. σ-Cu-ligand was gradually decreased with the decrease of phenolic compounds and thus dual-reaction center played a vital role in a catalytic reaction. More hydroxyl radicals are being generated by reduction of H_2O_2 by electron-rich Bi center and oxygen vacancies formed in $Bi_{12}O_{15}Cl_6$ during the calcining process. Due to these synergetic effects high catalytic efficiency has been reported.

$CuBi_2O_4$ and its composites with α-Bi_2O_3 were constructed by the sol-gel method which exhibited the brilliant and stable catalytic activity in sulfate radical-photo-Fenton process for the degradation of rhodamine B. SR-photo-Fenton reaction is an amalgamation of interface and solution reactions. In the interface reaction, the transfer of photogenerated electron/hole pairs drives the decomposition of PMS to produce SO_4•$^-$ and •OH which were confirmed by radical quenching and EPR experiments.

Another efficient Fenton - like catalyst was developed by Prem Kumar [24] using bimetallic iron and copper oxide nanoparticles supported on hydroxylated diamond (D3). This catalyst has shown appreciable stability and sustainability at pH 6. Due to the synergetic effect of high activity of Cu (I) to decompose H_2O_2 to hydroxyl radical and regeneration of these reduced copper species by ferrous ions.

$LaCuO_3$ perovskite catalyzed photo Fenton-like oxidation of food dye Tartrazine was investigated by Palas et al. [25] under visible and UV light irradiation where 83.9% and 90.2% decolorization was reported under visible and UV light irradiation, respectively. A good amount of degradation was also achieved. At optimum reaction conditions, 5.9% *Lepidium sativum* root growth inhibition was also observed by which toxicity was measured.

Improved Fenton-like catalytic activity of Cu-g-C_3N_4 composite was reported by Zhu et al. [26] for degradation of organic dyes. This catalyst was fabricated by pyrolyzing a melamine template crystalline copper chloride $[H_2mela]_2[CuCl_5]Cl$ where high content of Cu–N_x species was well dispersed in the Cu-g-C_3N_4 composite.

Cu_2O/H_2O_2 heterogeneous Fenton process was applied to encourage the degradation degree of CODs in the pulp wastewater in the ceramic membrane reactor by Zhou et al. [27] The catalyst recyclability was also assessed in a five-cycle test.

Soltani and Lee [28] investigated the degradation of 2-chlorophenol by photo Fenton process using three metal-doped BiFeO3 magnetic nanoparticles [$Bi_{1-x}Ba_xFeO_3$, $BiFe_{1-y}Cu_yO_3$, and $Bi_{1-x}Ba_xFe_{1-y}Cu_yO_3$], which were synthesized by sol-gel method. It was observed that Fe^{3+}/Fe^{2+} and Cu^{+}/Cu^{2+} pairs in the BFO magnetic nanoparticles systems effectively decomposed H_2O_2 to hydroxyl radicals and $S_2O_8^{2-}$ to sulfate radicals. It was reported that Cu-doped BFO ($BiFe_{1-y}Cu_yO_3$) and Ba-Cu co-doped BFO ($Bi_{1-x}Ba_xFe_{1-y}Cu_yO_3$) almost completely degraded 2-CP in 70 min. it was concluded that due to the formation of OH and SO4- in the $Cu^{2+}/Fe^{2+}/H_2O_2$/visible light couple and $Cu^{2+}/Fe^{2+}/S_2O_8^{2-}$/visible light couple, respectively high degradation of 2-CP was observed.

Mesoporous CuTUD-1 was synthesized by hydrothermal, surfactant-free route using tetramethylene glycol as a structure-directing agent by Pachamuthu et al. [29] The Fenton-like catalytic activity of this catalyst was assessed by the degradation of bisphenol A where high degradation was observed with negligible metal leaching.

2.2 Manganese (Mn) based catalyst

An efficient Fenton-like process was developed by Lai et al. [30] for the degradation of tetracycline at circumneutral pH by using $MnFe_2O_4$ nanoparticle and $MnFe_2O_4$/bio-char composite with different bio-char contents which can be easily separated from the solution by an external magnetic field. The biochar played a crucial role to suppressed the aggregation of $MnFe_2O_4$ and significantly increased the specific surface area. Here both the metal Fe and Mn ions at the same time participate in the activation of H_2O_2. This catalyst was found to be very stable and negligible leaching of metal ions was observed.

Cui et al. [31] designed the novel biomass route to fabricate active carbon fibers-based micromotors whose surface is decorated with Mn_3O_4 nanosheets coated ZnO nanorods. Here, Mn_3O_4 acts as a Fenton-like catalyst. ACFs can play various roles as it acts as an absorbent to condense organic pollutants on the surface, to ease out the formation of hydroxyl radicals it can be electron transfer mediator and for expediting the light-harvesting it provides support for the high dispersion of Mn_3O_4@ZnO heterojunction. Because of these reasons a high catalytic activity was reported.

Wang et al. [32] made an investigation in the field of the metal-organic framework modified spinel bimetallic oxides in heterogeneous photo-Fenton reactions. Zeolite imidazole framework-8-modified $MnFe_2O_4$ magnetic catalyst was prepared and its catalytic activity was assessed by photo-Fenton degradation of TC. The increased efficiency of catalyst can be attributed to the formation of Zn-O-Fe structure by ZIF-8-modified $MnFe_2O_4$ which promotes the crystalline structure, increase the light-harvesting and encourage the formation as well as the separation of the photo-induced carrier.

Fe, Mn co-supported SAPO-18 zeolite was synthesized by Li et al. [33] using the ion-exchange method. Fe-Mn/SAPO-18 demonstrated high performance in catalytic degradation of methyl orange. The enhancement in the generation of the hydroxyl radicals and thus the degradation efficiency can be explained on basis of synergism between Fe and Mn.

Ni et al. [34] studied the spinel-type cobalt-manganese oxide catalyzed degradation of Orange II. This catalyst was prepared in a two-step oxidation-precipitation method at modest temperatures. This catalyzed was employed in presence of $NaHSO_3$ and light to degrade orange II. The expedient degradation can be attributed to the generation of active species such as Mn (III), holes, and sulfate and hydroxyl radicals**.**

Lai et al. [35] synthesized stable and magnetically separable $MnFe_2O_4$/bio-char composite and examined the Fenton–like catalytic activity for the degradation of tetracycline at neutral pH. The enhanced activity could be attributed to the greater specific surface area due to biochar which effectively suppressed the aggregation of $MnFe_2O_4$ and simultaneous participation of both Fe and Mn ions in the activation of H_2O_2. Various transition metal nanocomposites oxide MnO_2/NiO were prepared by a hydrothermal method using different nickel oxide to manganese oxide ratios and their heterogeneous Fenton-like catalyst activity was evaluated for the degradation of dye Orange II using $NaHSO_3$. An excellent OII removal efficiency, good stability, and recovery performance was reported for the MnO_2/NiO nanocomposite (Ni: Mn = 1:2) [36].

The magnetically separable $MnFe_2O_4$ nanoparticles were prepared onto SnS_2 micro flowers through a two-step hydrothermal process by Zhao et al. [37] Due to efficient separation of photoexcited electron/hole pairs high photocatalytic performance of this catalyst was reported for the degradation of methylene blue. It was concluded that as the result of the Z-scheme electron transfer, Mn^{2+} and Fe^{2+} in-situ regenerated through accepting electrons from the cathode.

A reduced graphene oxide (RGO)-supported $CoMn_2O_{3.5}$ composite i.e. $CoMn_2O_{3.5}$-RGO, a Fenton-like catalyst was synthesized by Qu et al. [38] using the coprecipitation method, where RGO sheets were decorated with $CoMn_2O_{3.5}$ nanoparticles and self-organized into microcubes. The photocatalytic activity was assessed for the decomposition of various dyes including methylene blue, rhodamine B, and golden orange II. The improved activity of the catalyst was attributed to a synergistic effect of RGO and $CoMn_2O_{3.5}$, where the dyes are adsorbed on the surface of RGO by interaction and retained in close vicinity to the active sites of $CoMn_2O_{3.5}$.

MnO_2-templated iron oxide-coated diatomites were investigated for their catalytic performance in heterogeneous photo Fenton-like systems by He et al. [39]. These catalysts were fabricated via hydrothermal synthesis and sacrificial template redox etching reaction. Here, Fe_2O_3 nanorods were uniformly distributed on the surface of diatomite. The change in the morphology of FeOOH from nanorods into nanoflowers was reported when the reaction time was prolonged from 12 h to 24 h. By the FeOOH@diatomite samples, calcined under different atmospheres, two different crystal phases of Fe_2O_3@diatomite were achieved. An excellent degradation efficiency, stability, and reusability were observed for the degradation of methylene blue by α-Fe_2O_3@diatomite composites.

A Magnetic recyclable ternary nano photocatalyst $MnFe_2O_4/CeO_2/SnS_2$ was synthesized by Zhao et al. [40] using a hydrothermal route. To prepare this catalyst $MnFe_2O_4$ and CeO_2 nanoparticles were decorated onto SnS_2 flowers where SnS_2 acts as a vivid connector between $MnFe_2O_4$ and CeO_2 with a suitable bandgap. This bandgap led to highly separated photogenerated electron-hole pairs and thus resulted in expedient degradation of methylene blue. The coexistence of Mn^{2+}/Mn^{3+} and Fe^{3+}/Fe^{2+} redox couples were reported.

Wang et al. [41] studied the sulfate radical-based photo-Fenton-like degradation of antibiotic levofloxacin using the H2-reduced mesoporous MnO@MnOx microspheres and peroxymonosulfate (PMS) as an oxidant. It was observed that in the SR-photo-Fenton-like oxidation process several species like $SO_4^{\bullet-}$, $^{\bullet}OH$, $O_2^{\bullet-}$ and $^1O_2$ played a crucial role. High efficiency, improved stability, and negligible Mn-ions leaching was reported which can be attributed to the mesoporous structure and multivalence and oxygen vacancies which led to the large specific area, more absorbance of UV–vis radiation, effective charge separation in combination with required self-redox properties of Mn-ions on the surface of the catalyst.

The Fenton-like reaction using activated alumina supported CoMnAl composite metal oxides catalyst for detoxification of pharmaceutical wastewater at neutral or slightly basic pH was demonstrated by Ling et al. [42]. Synergism between Co and Mn on the surface of the catalyst caused more generation of hydroxyl radicals.

Ferrum manganese oxide nanosheets were developed on the microchannels of carbonized wood to construct a three-dimensional wood-derived block for proficient wastewater treatment by Xia et al. [43]. Several important roles of carbon were identified such as provide support Fe-Mn-O NSs, contributes to unimpeded mass diffusion benefiting from the various open channels and hierarchical pores on channel walls. By doping alien-metal elements some of the important surface properties like surface defects, surface charge, low-valence metal concentration, and charge transfer were improved which in turn resulting in high Fenton activity and stability.

A promising Fenton-like catalyst metal-doped zinc ferrite nanosphere was fabricated by Li et al. [44] from metal-rich industrial wastewater using a two-step method. The high photocatalytic degradation of Cango red was reported. It was observed that Cr and Mn doping boosted the photocatalytic activity of $ZnFe_2O_4$.

The outstanding removal efficiency of Tetrabromobisphenol A was reported by He et al. [45] using nanoscale zerovalent iron-loaded magnetic bimetallic hollow Fe0@C@$MnFe_2O_4$ sphere as a Fenton-like catalyst. In the preparation scheme, the carbon shell of polydopamine was fabricated via self-oxidation of dopamine by adding $MnFe_2O_4$ hollow spheres into dopamine solutions. This mesoporous structure causes high adsorption capacity for concentrating TBBPA around the catalyst which resulted in high degradation efficiency. A one-pot solvothermal method was used to prepare this catalyst. To achieve active nZVI in-situ, Fe2+ ions were adsorbed on the surface of PDA@$MnFe_2O_4$ followed by calcination. The photocatalytic activity of this catalyst was evaluated for the degradation of TBBPA where high degradation capacity, easy magnetic separation, and high recyclability were recorded.

The photo-Fenton-like process was developed by Wang et al. [46] for the removal of fluoroquinolone antibiotics using mesoporous manganese oxide microsphere synthesized via soft-template P123 assisted method. An expedient removal of ofloxacin, ciprofloxacin, enrofloxacin, and levofloxacin was reported using P2-Mn_3O_4, peroxymonosulfate under UV irradiations.

An attempt is made for the first time to modify Chitosan by 3,5-Dinitrosalicylic acid by Shoueir et al. [47] to prepare DNSA@CS@$MnFe_2O_4$ nano photocatalyst. DNSA@CS serves as a brilliant connector between methylene blue and MnFe2O4 which enhance both adsorption and photodecomposition under visible light and thus accelerate the rate of photo-Fenton degradation. The hybrid DNSA@CS@$MnFe_2O_4$ mechanism was explained based on the coexistence of Mn^{2+}/Mn^{3+} and Fe^{3+}/Fe^{2+} redox couples.

Chen et al. [48] synthesized a hollow Mn-doped Fe_3O_4/RGO hybrid by solvothermal method followed by a reduction of GO via $NaBH_4$. High stability, recyclability, degradation efficiency at neutral pH, and easy separation was reported for the rhodamine B degradation.

2.3 Cobalt (Co) based Fenton-catalyst

Mahamallik and Pal [49] investigated the degradation of textile wastewater by a modified photo-Fenton process using Co-SMA where Co(II) is adsorbed on the bilayer structure of sodium dodecyl sulfate formed on an alumina support.

Cobalt and chromium-containing layered double hydroxide (LDH) [CoCr-LDH and CoCr/Fe_3O_4-LDH] were fabricated with or without Fe_3O_4 and the effect of the addition of magnetite in LDH on the structure and catalytic activity was studied by Rosembergue Gabriel Lima Gonçalves. It was observed that magnetite incorporated and form a composite with magnetic property and endorsing modification in the morphology, quantity, and size of the LDH pores. An expedient performance for the degradation of reactive black can be attributed to the higher surface area and larger pores for Fe_3O_4/LDH which permits a more effective contact with the dye.

Hu et al. [50] prepared a new flower-like 3D hierarchical cobalt phosphate $Co_3(PO_4)_2{\cdot}8H_2O$ (fCoP), and a plate-like cobalt phosphate (pCoP) at low temperature under atmospheric pressure by a microwave-assisted technique using hexamethylene tetramine (HMTA) or urea as a template. Fenton-like and photo-Fenton-like catalytic activity of these catalysts were evaluated by using Rhodamine B as a model compound. Due to the flower-like hierarchical fCoP higher efficiency of the process was recorded. Here, superoxide radical ($^{\bullet}O_2^-$) was found to be the prevailing active species in the Fenton-like processes.

Cheng et al. [51] came up with a novel composite Fe/Co catalyst which was prepared through the modification of steel converter slag (SCS) by salicylic acid–methanol (SAM) and cobalt nitrate ($Co(NO_3)_2$). The prepared catalyst shows a very high efficiency of Fenton-like degradation of sulfamethazine (SMZ). The observed degradation rate of SMZ in Co-SAM-SCS/H_2O_2 system was 2.48, 3.20, 6.18, and 16.21 times of that in Fe-SAM-SCS/H_2O_2, SAM-SCS/H_2O_2, $Co(NO_3)_2/H_2O_2$, and SCS/H_2O_2 system, respectively at initial pH of 7.0. The enhanced activity can be attributed to the synergism between Co and SAM-SCS and high surface area.

Mesoporous bimetallic Fe/Co was prepared by employing a nano casting strategy with KIT-6 as a hard template by Li et al. [9]. This catalyst exhibited excellent catalytic efficiency, good stability, and reusability for the degradation of tetracycline hydrochlorides via a Fenton-like process operating at a wider pH range.

2.4 Nickel (Ni) based Fenton-catalyst

Magnetic nickel ferrite particles were prepared by using iron-containing sludge via a co-precipitation method followed by sintering at 800°C. An excellent photo Fenton-like activity was reported for removal of phenol which can be attributed to the rapid electron exchange between Ni II and Fe III ions in the NiFe2O4 structure.

To fabricate $NiFe_2O_4$ and Mg-doped ferrite photocatalysts a green sol-gel route was implemented by Nadumane et al. [8] where Aloe Vera gel is used. The enhanced photocatalytic activity was reported for the decomposition of recalcitrant pollutants due to the balance between the parameters, crystallinity, bandgap, morphology, crystallite size, defects, dopant amount, and combined facets of photocatalysis.

Han et al. [52] devised a low-cost method for the fabrication of spinel-type $Ni0.63Mg0.30Cu0.07Fe_2O_4$, a Fenton-like catalyst by using nickel sulfide via an acid leaching-coprecipitation-calcination method. The photo-Fenton-like catalytic property was evaluated for the degradation of Rhodamine B (RhB) assisted by oxalic acid ($H_2C_2O_4$) where 97.25 degradation efficiency and 85.65% total organic carbon removal efficiency in 90 min was reported.

A novel ternary solid solution Fe_7Ni_3S was prepared and used as a photo-Fenton catalyst for the degradation of Rhodamine B and TTCH under UV and Visible light at neutral pH by Shao et al. [53] In this study. the phase transformation from marcasite-FeS_2 to millerite-NiS was achieved. By using density functional theory the electronic structures were calculated and acid-base buffer function for photo-Fenton degradation of organic pollutants was explained.

3. Graphene oxide/Carbon/CNT

Gong et al. [54] synthesized a novel core-shell structured Fe_3O_4@GO@MIL-100(Fe) magnetic catalyst was and employed it as a heterogeneous photo-Fenton catalyst for the degradation of 2,4-dichlorophenl (2,4-DCP) where almost 100% degradation of 2,4-DCP within 40 min was reported. This high efficiency was explained based on the efficient transfer of photo-generated electrons between MIL-100(Fe) and Fe_3O_4 by GO. Good stability and recoverability were reported.

Wang et al. [55] assessed the effect of various reaction parameters on the degradation of phenol by RGO/α-FeOOH supported on Al-MCM catalyst in the heterogeneous photo-Fenton system. They also studied the effect of the addition of anions (Cl^-, SO_4^{2-}, NO_3^-, HCO_3^-, HPO_4^{2-}), small molecule organic acids (CA, OA, TA), and natural organic matter (HA, FA) and observed the inhibition effect on phenol degradation.

Yu et al. [56] studied the degradation of phenol employing Graphene oxide–iron oxide (Fe3O4-GO) nanocomposites as heterogeneous photo-Fenton catalysts which were synthesized via co-precipitation combining hydrothermal method. Hybridizing zero-dimensional nanoparticles with two-dimensional graphene oxide nanosheets was proven to be an efficient way to increase adsorptive and catalytic performance. High catalytic activity was observed even after five cycles. It was concluded that because of GO the adsorption capacity was increased, more active sites were available and triggered the Fe^{3+}/Fe^{2+} cycle.

A novel graphene oxide/MIL-88A(Fe) (GO/M88A) membrane was prepared via facile vacuum filtration method by Xie et al. [57] and photo-Fenton-like catalytic activity was assessed. It was observed that the intercalation of photo-Fenton catalytic M88A into GO nanosheets regulated 2D nanochannels as well as endow the membrane with photo-Fenton catalytic activity. This GO/M88A membrane exhibited excellent separation performance and stability. It was proven as an efficient catalyst to treat real textile wastewaters and to degrade contaminants like MB, BPA.

TiO_2-graphene oxide (GO)-Fe_3O_4 was fabricated by Li et al. [58] which exhibited expedient photo-Fenton catalytic activity and stability for the degradation of amoxicillin. For the recovery of the catalysts, the combination of a submerged magnetic separation membrane photocatalytic reactor (SMSMPR) and TiO_2-GO-Fe_3O_4 was applied. It was reported that GO persuaded better cycle and catalytic performance of the catalysts whereas Fe_3O_4 enhance the heterogeneous Fenton degradation of organic compounds and endow the magnetism of the photocatalyst for magnetic separation from treated water.

Jin and Dong [59] designed a strategy to combine visible-light photocatalytic oxidation (Vis-Photo) and sulfate-based ($SO_4^{\cdot-}$) heterogeneous Fenton-like reaction (SR-Fenton) in form of a novel system of Ag_3PO_4/Fe_3O_4/GO bifunctional catalysts. The enhanced catalytic activity was reported for p-chlorophenol degradation which can be attributed to synergism between the catalysts.

Transformation pathway and mechanism of degradation of methylene blue using the β-FeOOH@GO catalyzed photo-Fenton-like system was proposed by Su et al. [60] The akaganéite nanoparticles, rice spike-like akaganéite impregnated graphene oxide (β-FeOOH@GO) nanocomposite was prepared through facile hydrolysis. For β-FeOOH@GO catalyzed photo Fenton-like system the complete elimination of MB and its acute toxicity to Luminous bacteria was reported. The mechanistic study revealed that MB degradation pathway primarily continued with the breaking of phenothiazine rings oxidized with $^{\bullet}OH$, $HO_2^{\bullet}$, and singlet oxygen radicals. Here for the first time, sulfoxide intermediates, sulphone intermediates, and desulfurization intermediates, and N-demethylation or dimethamine intermediates were reported.

To fabricate hybrid nanocomposite (Pb-BFO/rGO) Pb-doped $BiFeO_3$ (BFO) nanoparticles were grafted on reduced graphene oxide (rGO) sheets using a microwave-assisted hydrothermal method and photo Fenton like catalytic activity was evaluated for the decomposition of perfluorooctanoic acid (PFOA) by Li et al. [61] Enhanced catalytic efficiency of Pb-BFO/rGO can be ascribed to the large specific surface area, small crystallite sizes and multiple functional groups such as carboxyl groups and Fe-O groups. In addition to this irradiation with microwave caused energy transfer and cross-coupling reactions which significantly influence the degradation of PFOA where Pb-BFO/rGO absorbed the microwave energy, which facilitated the decomposition of H_2O_2 and the generation of hydroxyl radicals. Liu et al. [62] fabricated α-Fe_2O_3 anchored on graphene oxide (α-Fe_2O_3@GO) through the facile hydrolysis method. The high photo-Fenton-like catalytic activity for the degradation of organic compounds can be ascribed to the unique incorporation of GO into the catalyst which mediated the morphology of active sites α-Fe_2O_3 nanoparticles and also offered high electron conductivity and electrostatic attraction between negatively charged GO with positively charged MB.

An attempt has been made by Xu et al. [63] to anchored magnetite nanoparticles on to graphene layer. Magnetic Fe_3O_4 and reduced graphene oxide (RGO) nanocomposites were prepared by a facile alkaline-thermal precipitation method. Without using any additional reducing agent in one pot the anchoring of Fe_3O_4 NPs and the reduction of GO were achieved. This prepared ferromagnetic catalyst exhibited high efficiency for the degradation of methyl orange.

Liu et al. [64] reported that aligned α-FeOOH nanorods anchored on a graphene oxide-carbon nanotubes aerogel fabricated through Fe^{2+} induced reduction self-assembly process can function as an effective Fenton-like oxidation catalyst. The high efficiency can be attributed to the three-dimensional porous aerogel network which facilitates efficient charge/mass-transfer and the efficient conversion between Fe^{2+}/Fe^{3+} and synergistic coupling between α-FeOOH and carbon-based aerogel matrix. For assessing the catalytic activity various organic compounds like Orange II (OII), rhodamine B (RhB), methylene blue (MB), phenol, and endocrine disruptor bisphenol A (BPA) were used.

Nanoscale zero-valent iron particles stabilized by sulfur/nitrogen dual-doped r-GO (nZVIPs@SN-G) were prepared by Ma et al. [65] and catalytic activity was tested for the degradation of 2,4-dichlorophenoxyacetic acid.

Nguyen et al. [66] proposed the modified graphene oxide-based Fenton process for the degradation of Metaldehyde. Single-layer graphene oxide (SLGO) having higher hydrophilic nature takes part in a redox reaction with hydrogen peroxide and can stabilize the $\cdot OH$ generated, which leads to degradation of organic contaminants.

Zhu et al. [67] fabricated the novel and highly efficient heterogeneous Fenton catalysts (CNTs/Fh) by coupling the oxidized multi-walled carbon nanotubes with ferrihydrite. Due to acceleration of the electron transfer from H_2O_2 to Fh and lowering of Fe(III)/Fe(II) redox potential, the Fe(III)/Fe(II) redox cycling on CNTs/Fh considerably improved during the Fenton reaction which was proven by density functional theory calculations and the cyclic voltammograms curves.

Nitrogen-doped carbon nanotubes-FePO4 composite from phosphate residue was synthesized by surface modification and chemical vapor deposition and its application as an effective Fenton-like catalyst for the degradation of Rhodamine B was observed by Wei et al. [68].

Liu et al. [69] fabricated a novel Fenton-like catalyst (Zn-Fe-CNTs) employing an infiltration fusion method followed by chemical replacement in an argon atmosphere. The Fenton-like activity of this catalyst was demonstrated for the degradation of sulfamethoxazole (SMX). The high efficiency of catalyst can be explained on the basis of the coral porous structure of Zn-Fe-CNTs with a BET area of 51.67 m^2/g, demonstrating excellent adsorption capacity for SMX. Zn^0 and Fe^0/Fe_2O_3 were observed on the surface of Zn-Fe-CNTs. By micro-electrolysis it can reduce O_2 into H_2O_2 and Fe^0/Fe_2O_3 could catalyze the in-situ generation of H_2O_2 to produce hydroxyl radicals.

By physical activation/ chemical activation methods an AC was prepared from walnut shells by Tekin et al. [70]. On this 10%, Fe or 10% Fe-TiO_2 catalysts were loaded. The activity of this prepared catalyst was demonstrated for the degradation of benzoic acid.

A novel α-FeOOH/mesoporous carbon (α-FeOOH/MesoC) composite as a heterogeneous Fenton-like catalyst with high stability and efficiency was fabricated via in situ crystallization of adsorbed ferric ions within carboxyl functionalized mesoporous carbon. In this catalyst, visible light active α-FeOOH nanocrystals were caged in the mesoporous frameworks. Due to synergism between α-FeOOH and MesoC in α-FeOOH/MesoC composite enhanced the mineralization efficiency for the degradation of Organic Pollutant [71].

Miao et al. [72] achieved tuning layered Fe-doped g-C3N4 structure which can work as an efficient Fenton catalyst. By following the bottom-up strategy various iron-doped g-C_3N_4 compounds were synthesized and then split from the bulk structure into a multi-layer structure with uniformly dispersed mesopores by controlled pyrolysis.

An attempt has been made by Long et al. [73] to improvise the Fe(III)/Fe(II) cycle by preparing a Fenton-like catalyst where nano-Fe° were encapsulated in hydrothermal carbon (Fe°/HTCC). A high degradation efficiency was reported for the degradation of p-chlorophenol in presence of light.

Greater activity, higher stability, and recyclability for Fe_{ox} NPs supported on the hydroxylated surface of modified diamond nanoparticles (D3) was reported by Espinosa et al. [74].

$LaFeO_3$/C nanocomposite as efficient photo-Fenton-like catalyst was developed for the degradation of Rhodamine B by Wang et al. [75]. Here $LaFeO_3$ nanoparticles were immobilized by ultrasonic-assisted surface ions adsorption method on the surface of monodisperse carbon spheres. Due to the high specific surface area; synergism between the presence of monodisperse carbon spheres and photo-Fenton-like process a higher catalytic activity was observed.

Zou et al. [76] doped Iron oxide onto fullerene[60] (C60) to form a C60-Fe2O3 composite via the impregnation method. The Fenton like activity of the prepared catalyst was evaluated for the degradation of methylene blue, rhodamine B, methyl orange, and phenol. The enhanced activity was reported for fullerene[60]-iron oxide complex over a wide pH range 3.06–10.34.

The degradation of methylene blue and congo red was examined by Saleh and Taufik [77] using Fenton, photo-Fenton, sono-Fenton, and sonophoto-Fenton methods in presence of Fe_3O_4/ZnO/graphene composites. This catalyst was fabricated by the hydrothermal method and exhibited high stability even after four cycles because of the incorporation of graphene.

Fenton-like degradation of ofloxacin was reported for sludge-derived carbon (SC) by Yu et al. [78]. Enhanced catalytic activity was observed for the sulphuric acid-treated SC which causes low pH of the surface.

Photo-Fenton degradation of rhodamine B was reported by employing reduced graphene oxide nanosheet/Fe_xO_y/nitrogen-doped carbon layer (rGS/Fe_xO_y/NCL) aerogel. This rGS/Fe_xO_y/NCL catalyst was prepared by a redox reaction followed by calcination where Fe_xO_y NPs sandwiched between rGS and NCL [79].

Wen et al. [80] synthesized the carbon encapsulated Fe nanoparticles by carbonization of pretreated sludge precursors which was obtained by radical assisted iron impregnation. Resulted products characterized with much higher iron insertion rate and the uniformly dispersed Fe NPs encapsulated into porous carbons. A higher Fenton like catalytic activity was observed for the degradation of Black-T.

Li et al. [81] suggested the synthesis of biomass tar-based monometallic (Fe/C) and bimetallic (FeNi/C) Fenton-like catalytic nanoparticles using ball milling combined with calcination. Greater efficiency was exhibited by the bimetal catalyst prepared at 300 °C (FeNi/C-300) for degradation of MB because of enhanced electron exchange due to the introduction of nickel and the formation of defective graphite layers.

Oruç et al. [82] also proposed the synthesis of biomass-derived activated carbon/Fe-Zn bimetallic nanoparticles in which lemon (Citrus limon (L.) Burm. f.) wastes were utilized for the preparation of efficient catalysts and employed for the degradation of azo-dye Reactive Red 2.

Guo et al. [83] prepared the novel graphite carbon coating hollow $CuFe_2O_4$ spheres by a solvothermal method and catalytic performance was assessed in photo-Fenton-like degradation of methylene blue (MB). H-CFO@C-600 °C-0.15 SPs exhibit excellent catalytic activity which can be attributed to the efficient separation and transfer of photoinduced electrons accelerated the enhancement of catalytic activity.

Amorphous FeOOH quantum dots (QDs) were anchored on polymeric photocatalysts *g*-C_3N_4 which were used as a photo-Fenton catalyst by Qian et al. [84]. XPS study revealed the presence of extraneous carbon species in FeOOH/*g*-C_3N_4 which could be responsible for the electron transfer between FeOOH and *g*-C_3N_4. The beneficial interaction of FeOOH QDs and carbon species resulted in inhibited leaching of iron.

Ye et al. [85] fabricated the Z-scheme g-C_3N_4/$LaFeO_3$ heterojunctions by calcining the uniformly mixed g-C_3N_4 nanosheets and $LaFeO_3$ nanoparticles. In this prepared catalyst, $LaFeO_3$ nanoparticles were found to be uniformly assembled onto the surface of g-C_3N_4 nanosheets through chemical bonding. The catalytic performance was demonstrated for the degradation of dye RhB. Z-scheme electron transfer and the synergistic effect between $LaFeO_3$ and g-C_3N_4 led to enhance photo-Fenton activity.

Bicalho et al. [86] demonstrated the high efficiency of Fe(II)-doped g-C_3N_4 for the Fenton like degradation of methylene blue, rhodamine B, anionic indigo carmine (IC), and neutral phenol. This catalyst was synthesized by simple calcination of a Fe^{+3}/melamine precursor.

Fe_3O_4/g-C_3N_4 nanoparticles were prepared via electrostatic self-assembly method by Sahar et al. [87]. Several advantages like a high surface area, efficient charge transfer between Fe_3O_4 and g-C_3N_4 at the heterojunctions, inhibition of electron-hole recombination, and stabilization of Fe_3O_4 against leaching by the hydrophobic g-C_3N_4 were reported which resulted into high catalytic performance for the degradation of Rhodamine B.

He et al. [88] fabricated the ternary g-C_3N_4/Ag/γ-FeOOH catalyst and reported the photo-Fenton-like catalytic activity for the degradation of methyl orange.

By microwave hydrothermal method hybrid catalysts ($Zn_{0.94}Fe_{0.04}S$/g-C_3N_4 or ZCN) were developed by Wang et al. [89] and employed for the degradation of *p*-nitrophenol. This study showed that the deposition of Fe-doped ZnS onto g-C_3N_4 sheets prohibited the aggregation of $Zn_{0.94}Fe_{0.04}S$ and increased the surface area.

Heterogeneous Fenton platform was constructed by the chemical embedding of carbon nanodots onto the surface of iron oxychloride (FeOCl/CDots) by Zhang et al. [90]. Here, carbon dots acted as the reactive sites for highly effective separation of photogenerated electrons and holes in the FeOCl substrate. On the carbon dots, O_2 molecules reduced to H_2O_2 and FeOCl substrate with abundant Fe^{2+} could directly capture and activate the H_2O_2 to produce abundant hydroxyl radical ($\cdot OH$).

The one-pot method was designed by Shao et al. [91] to prepare a well-dispersed Fe_3O_4-doped ordered mesoporous carbon catalyst supported on porous sintered metal fibers and its Fenton-like activity was evaluated and a comparative study was made for degradation of phenol. It was found that this catalyst is more efficient than the Fe-OMC pellet catalyst in terms of catalytic activity, stability, and leaching of iron.

Cu based Fenton like catalyst was developed by Ma et al. [92] where reduced Cu was firmly embedded in the g-C_3N_4 sheet. Here cuprous ion achieved stability by strong coordination with pyridinic N. The prepared catalyst exhibited improved catalytic performance in the degradation of Rhodamine B. Hydroxyl radicals and singlet oxygen was reported as active species which were generated by the reaction of the cuprous ion with hydrogen peroxide and the resulting cupric ion can easily be reduced because of higher stability of cuprous ion.

An et al. [93] fabricated polyoxometalates/oxygen doped g-C_3N_4 nanocomposites. In the comparison of pristine carbon nitride, this catalyst exhibited superior Fenton like catalytic activity for the degradation of sulfosalicylic acid. Oxygen doping of C_3N_4 was proven advantageous for the formation of strongly coupled heterointerfaces which in turn play important role in interfacial charge transfer for oxygen activation and surface activation of oxygen molecules.

Fenton-like degradation of ciprofloxacin over g-C_3N_4-iron oxide composite was reported by Ding et al. [94]. This catalyst was prepared by synthesizing g-C_3N_4 in-situ onto iron oxide where iron oxide NPS were intercalated into the layers of g-C_3N_4 which lead to high surface area and more stability and thus better catalytic activity was shown.

Another Fe-doped g-C3N4 catalyst was prepared by Hu et al. [95] via thermal shrinkage polymerization and used to degrade phenol, bisphenol A, 2, 4-dichlorophenol, and complex coking wastewater. Immobilization of iron was achieved by σ-π bonds.

Fe-g-C_3N_4/graphitized mesoporous carbon composite was fabricated by Ma et al. [96] and its Fenton-like catalytic activity was assessed for the degradation of Acid Red 73 as a model compound over a wide pH range of 4–10. It was reported that Fe-N species are the most important active sites.

By one-step pyrolysis of Fe-metal organic frameworks and montmorillonites, core/shell type Fe^0@carbon nanocomposites were inserted in the interlayer space of MMT and employed for the degradation of phenol and methyl orange [97]. By study it was observed that montmorillonites accelerate release Fe^{2+} and influence capture of electrons by H_2O_2 and capable of adjusting pH of the solution by itself and show high catalytic activity and stability.

4. MIL / MOF

Li et al. [98] prepared g-C_3N_4/NH_2-Iron terephthalate metal-organic framework heterojunction (g-C_3N_4/NH_2-MIL-88B(Fe)) hydrothermal method. This Fenton-like catalyst was employed for the degradation of methylene blue where 100% degradation was achieved and the synergy index of the lp-2 / visible light / H_2O_2 system was increased by 305%. The high efficiency can be attributed to inhibited recombination of photo-induced e^--h^+ pairs and expedited OH radical generation on the lp-2.

Wang et al. [99] reported an expedient degradation of TC by Zeolite imidazole framework-8-modified $MnFe_2O_4$ catalyst over a wide pH range. By following the one-step method this magnetic catalyst was prepared. Due to Zn-O-Fe structure, crystal formation and generation of photo- electron-hole got facilitated and high absorption of light was also achieved.

Fu et al. [100] designed the pathway for the synthesis of iron-based MOF, MIL-88A at room temperature and employed it as a photo-Fenton degradation of RhB and BPA. Here role of water in synthesis was identified and it was concluded that water assists the deprotonation of fumaric acid as well as in hydrolysis of iron salt to accelerate crystal nucleation.

Ahmad et al. [101] worked to tune the Lewis acidity of MIL-88B-Fe with mix-valence coordinatively unsaturated iron centers on ultrathin Ti_3C_2 nanosheets. This prepared novel photo-Fenton CUCs-MIL-88B-Fe catalyst exhibited high-efficiency stability and reusability for the degradation of pollutants.

A stable magnetic MIL(Fe)-type MOF-derived N-doped nano-ZVI@C rods were fabricated by Ye et al. [102] and used as a heterogeneous catalyst for the electro-Fenton degradation of gemfibrozil. High catalytic activity was attributed to carbon doping with N and ZVI encouraged the incessant conversion of Ferric to ferrous in Fenton's reaction.

MOF [NH_2-MIL-101(Fe) was prepared hydrothermally and reported as a strong Fenton catalyst by Taha et al. [103] It has high adsorption capacity and Fenton-like catalytic activity. High efficiency was observed due to the synergism between the high adsorption, sustainable Fe ions release, and rapid electron transfer for the degradation of RhB at pH 7.2.

Mesoporous MIL-100(Fe) loaded with ZnO NS was fabricated using an in-situ self-assembly approach and employed for photo-Fenton like degradation of Phenol, bisphenol-A, and atrazine for the first time by Ahmad et al. [104] The greater efficiency was reported and explained on the basis of its microcellular structure. A higher charge separation efficiency was achieved by the introduction of a definite amount of ZnO NS and H_2O_2.

Wu et al. [105] used iron-based metal-organic frameworks for the degradation of tetracycline hydrochloride over a wide pH range due to solid acid catalysts. It was reported that the photo-Fenton system based on iron-oxo (Fe-O) clusters in frameworks the Fe(II)/Fe(III) cycle could be fastened up by visible light irradiations. Due to the largest specific surface area, pore-volume, most coordinatively unsaturated iron sites, and synergistic effect expedient catalytic performance was reported by MIL-101/H_2O_2/visible light system.

In the same line, Gao et al. [106] used iron-based metal-organic frameworks namely MIL-88B-Fe for Fenton degradation of phenol. Higher catalytic performance could be achieved due to the abundance of active sites, the flexible structure, and facilitated reduction of Fe (III) to Fe(II).

MacDonald et al. assessed the photo-Fenton activity for the degradation of methylene blue by MIL-47(V) and MIL-53(Al) and compared Cu/MIL-47. A comparative study was made by MacDonald et al. [107] for the degradation of methylene blue by Fe/MIL-47 MIL-53(Al), Cu/MIL-47, and Fe/zeolite-Y. It was found that Fe/MIL-47 gives higher TOC mineralization due to the incorporation of Fe species into MIL-47. This catalyst was prepared via incipient wetness impregnation.

Tang and Wang [108] fabricated Fe-based magnetic nanoparticles embedded into mesoporous carbon from Fe-based metal-organic framework MIL-100(Fe) by a pyrolysis method. The Fenton-like catalytic activity was evaluated for the degradation of sulfamethoxazole for the first time where a high rate was reported. Enhanced catalytic performance could be attributed to the excellent enrichment ability of the outer mesoporous carbon matrix, the abundant active sites of the inner Fe-based NPs, and the synergistic effect between the two components.

Martínez et al. [109] constructed Fe-based MOF materials like SUST/Fe-BTC and MIL-100(Fe) at room temperature using water as a solvent under sustainable conditions. The catalytic activity was assessed for the degradation of methylene blue where SUST/Fe-BTC exhibited excellent results.

Mei et al. [110] explored the employability of modified MIL-53(Fe) using xylitol and D-sorbitol for the photo-Fenton-like degradation of pesticides like Thiamethoxam. By these compounds electronegativity of Fe-O clusters and surface area of MIL-53(Fe) was regulated. Here, due to the addition of Xylitol, the ratio of Fe^{II}/Fe^{III} decreased which results in the lower electron density around Fe atoms.

Another study is made by Nguyen et al. [111] using Composite photocatalysts containing MIL-53(Fe) for the photo-Fenton-like degradation of rhodamine B. these composites were prepared by Fe_3O_4 or $NiFe_2O_4$ with MIL-53(Fe). By comparative study, it was concluded that Fe_3O_4/MIL-53(Fe) samples have greater catalytic activity than that of the bare of Fe_3O_4, $NiFe_2O_4$, and MIL-53(Fe).

A bifunctional catalyst was synthesized by carbonization of iron-based MOFs by Cao et al. [112] where FeOx nanoparticles were embedded into N-doped hierarchically porous carbon (FeOx/NHPC). This catalyst exhibited high mineralization ability and high stability for the treatment of refractory wastewater containing phenol, sulfamethoxazole, atrazine, rhodamine B, and 2,4-dichlorophenol at neutral pH. By regulating N doping configurations and contents H_2O_2 production was improved and thus high catalysis performance was achieved.

Cheng et al. [113] reviewed the Metal-organic frameworks for heterogeneous Fenton-like catalysis where effects of pH on MOF-based Fenton-like catalysis and mechanism were elaborated.

Wang et al. [114] investigated the role of SnO2 shell in stabilizing the microstructure of Fe_2O_3. Prussian blue (PB) nanocubes were used as the precursor of porous Fe_2O_3 to prepare SnO_2-encapsulated α-Fe_2O_3 (Fe_2O_3@SnO_2) nanocubes by pre-coating Sn(OH)Cl on the surface of PB nanocubes. It was reported that SnO_2 shells could preserve the microstructure of Fe_2O_3 nanocubes and promote the phase variation of Fe_2O_3 from γ/β-phase to α-phase which exhibited greater photo-Fenton catalytic activity for the degradation of Rhodamine B (RhB).

Pan et al. [115] designed Cu-UiO-66 which is supported CuO catalysts on a metal-organic framework and employed as heterogeneous Fenton catalysts for the degradation of 4-chlorophenol which is Supported CuO catalysts on a metal-organic framework.

5. OXIDES

5.2 CeO_2

Huang et al. [116] fabricated novel heterogeneous $yCeO_2$/Fh by decorating bio-template synthesized ceria ($yCeO_2$) on Fh ($yCeO_2$/Fh). The catalytic activity was evaluated for the degradation of Tetracycline, Tetrabromobisphenol A, Rhodamine B, and 2,4-dichlorophenol. Higher degradation efficiency is achieved due to the introduction of $yCeO_2$ which enhanced the regeneration of Fe^{2+} and Ce^{3+} and Ce^{4+}/Ce^{3+} circulation, which further expedited H_2O_2 consumption.

Gogoi et al. [117] developed magnetically separable Fe_3O_4-CeO_2 metal oxide nanocomposite by coprecipitation method and applied it as a Fenton-like heterogeneous catalyst for degradation of catechol.

Fe_2O_3@CeO_2-ZrO_2/Palygorskite heterogeneous Fenton catalyst was synthesized by Ouyang et al. [118]. A higher catalytic efficiency was reported for the degradation of Cango red which could be attributed to the enhanced adsorption capacity and dispersibility of CeO_2-ZrO_2 and Fe_2O_3 nanoparticles, and charge transfer between these two species.

Eshaq et al. [119] constructed stable porous $FeVO_4$ nanorods decorated on CeO_2 nanocubes ($FeVO_4$@CeO_2) through hydrothermal route and used for sonophotocatalytic degradation of 4-nitrophenol (4-NP).

5.3 SiO_2

Fenton-like degradation of Reactive Red 24 was demonstrated using FeO-constituted iron slag (IS) wastes which have constituents like FeO, ZnO, and SiO_2 by Van et al. [120].

Qu et al. [121] fabricated a series of spinel ferrites magnetic nanoparticles $NiFe_2O_4$ by hydrothermal method followed by microemulsion method to achieve $NiFe_2O_4$@SiO_2. These magnetically separable catalysts were employed as heterogeneous Fenton-like catalyst for the degradation of Rhodamine B at neutral pH. An enhanced efficiency was reported for the $NiFe_2O_4$@SiO_2 than $NiFe_2O_4$.

Another efficient heterogeneous Fenton-like catalyst was developed by Du et al. [122] for the degradation of tetracycline over a wide pH range of 3-9. Yolk-shell structured Fe_3O_4@void@TiO_2 NPs were prepared by coating amorphous SiO_2 and TiO_2 shells around a Fe_3O_4 core through the sol-gel method to obtain Fe_3O_4@SiO_2@TiO_2, followed by crystallization of TiO2 and removal of SiO_2 via calcination and the ultrasonic ammonia-etching treatment, respectively. An expedient degradation is achieved due to the high crystallinity, superparamagnetic core, high specific surface area, efficient enrichment and confinement of reactants in the nanocavity of catalyst, synergism between TiO_2 shell and Fe_3O_4 efficient reduction of Fe^{3+} to Fe^{2+}.

Cohen et al. [123] employed γ-Fe_2O_3/SiO_2 microspheres as a heterogeneous Fenton-like catalyst for the degradation of methyl orange, methylene blue, and para-nitrophenol. Here, ring-hydroxylations and N demethylations were observed.

Zhou et al. [124] fabricated Fe_2O_3-SiO_2 photonic crystals with high accessible surface area and examined the photo-Fenton-like activity for the degradation of methyl orange. In comparison with macroporous or mesoporous Fe_2O_3-SiO_2 composites, commercial Fe_2O_3, and homogenous photo-Fenton system, these Fe_2O_3-SiO_2 photonic crystals exhibited remarkable high catalytic performance which could be explained on the basis of the outstanding adsorption of dye molecules by the hierarchical macro-mesoporous structure and superior light-harvesting achieved by coupling the absorption spectrum of methyl orange with the slow-light-effect region of the photonic crystal.

FeO_x, SiO_2, TiO_2/Ti photo-Fenton-like catalysts were constructed via PEO, and impregnation by Vasilyeva et al. [125] enhanced phenol degradation was observed for Fe-containing oxide coatings. By study, it was concluded that FeOOH-containing layers are more active than those containing Fe_2O_3.

Meng et al. [126] developed a one-pot synthesis method for the fabrication of Fe2O3 loaded SiO2 hollow particles followed by calcination and used as a photo-Fenton-like catalyst for the degradation of methylene blue. It was found that the silica layer could efficiently prevent the inner Fe_2O_3 nanoparticles from becoming large whereas citric acid endows stability to iron ions in ammonia solution.

Uma et al. [127] examined the photo-Fenton-like catalytic activity of prepared Ag-SiO_2@α-Fe_2O_3 nanocomposites sphere for the degradation of methylene blue. Excellent degradation efficiency can be attributed to the plasmonic effect of Ag metal under visible light irradiation.

Dispersible Fe_3O_4/SiO_2/C nanospheres were fabricated by Liu et al. [128]. The Fenton-like catalytic activity was assessed for the degradation of methylene blue over a wide pH range of 4–9. To prepare this catalyst the dispersible Fe_3O_4 cores were coated with SiO_2 and carbon.

Jia et al. [129] investigated the degradation of methyl blue (MB) and methyl orange (MO) dyes under various conditions by employing multifunctional Fe-based amorphous alloys with the nominal components of $Fe_{78}Si_9B_{13}$ and $Fe_{73.5}Si_{13.5}B_9Cu_1Nb_3$. The surface aging behavior of these alloys was studied and explained.

REFERENCES

1. Doan VD, Le VT, Le TTN, Nguyen HT (2019) Adv Mater Sci Eng :1–9. doi:10.1155/2019/5978149 .
2. Javaid R, Qazi UY (2019) Int J Environ Res Public Health 16:2066.
3. Bel Hadjltaief H, Sdiri A, Ltaief W, Da Costa P, Gálvez ME, Ben Zina M (2018) C R Chim 21:253.
4. Hussain S, Aneggi E, Briguglio S, Mattiussi M, Gelao V, Cabras I, Zorzenonb L, Trovarellia A, Goi D (2019) J Environ Chem Eng :103586. doi:10.1016/j.jece.2019.103586.
5. Feijoo S, González-Rodríguez J, Fernández L, Vázquez-Vázquez C, Feijoo G, Moreira MT (2019) Catalysts 10:23.
6. Zhang X, Geng Z, Jian J, He Y, Lv Z, Liu X, Yuan H (2020) Catalysts 10: 293.
7. Nadeem N, Zahid M, Tabasum A, Mansha A, Jilani A, Bhatti IA, Bhatti HN (2020) Mater Res Express 7: doi:10.1088/2053-1591/ab66ee.
8. Nadumane A, Shetty K, Anantharaju KS, Nagaswarupa HP, Rangappa D, Vidya YS, Nagabhushana H, Prashantha SC (2018) J Sci Adv Mater Dev 4:89.
9. Li J, Li X, Han J, Meng F, Jiang J, Li J, Xu C, Li Y (2019) Sci Rep 9: 15820.
10. Du W, Xu Q, Jin D, Wang X, Shu Y, Kong L, Hu X (2018) RSC Adv 8:40022.
11. Liu F, Ai J, Zhang H, Huang YH (2018) Environ Technol :doi:10.1080/09593330.2018.1505961.
12. Domenzain-Gonzalez J, Castro-Arellano JJ, Galicia-Luna LA, Lartundo-Rojas L (2019) Int J Photoenergy :1–15. doi:10.1155/2019/4981631.
13. Shaban M, Abukhadra MR, Ibrahim SS, Shahien MG (2017) Appl Water Sci 7:4743.

14. Yang X, Sun H, Zhang L, Zhao L, Lian J, Jiang Q (2016) Sci Rep 6: doi:10.1038/srep31591.
15. Frindy S, Sillanpää M (2020) Mater des 188:108461.
16. Wang L, Zhang Y, Li X, Xie Y, He J, Yu J, Song Y (2015) Sci Rep 5:doi:10.1038/srep14341.
17. Cheng M, Li Y, Huang D, Lai C, Zeng G, Huang J, Liu Z, Zhang C, Zhou C, Qin L, Xiong W, Yia H, Yang Y (2019) Chem Eng J 362:865.
18. Guo X, Wang K, Xu Y (2019) Mater Sci Eng 245B:75.
19. Ma P, Yu Y, Xie J, Fu Z (2017) Adv Powder Technol 28:2797.
20. Zheng C, Yang C, Cheng X, Xu S, Fan Z, Wang G, Wang S, Guan X, Sun X (2017) Sep Purif Technol 189:357.
21. Zhang Y, He J, Shi R, Yang P (2017) Appl Surf Sci 422:1042.
22. Subbulekshmi NL, Subramanian E (2017) J Environ Chem Eng 5:1360.
23. Xie Z, Zhou J, Wang J, François-Xavier CP, Wintgens T (2019) Appl Catal Environ 253B: 28.
24. Manickam-Periyaraman P, Espinosa JC, Ferrer B, Sivanesan S, Álvaro M, García H, Navalón S (2020) Chem Eng J 393:124770.
25. Palas B, Ersöz G, Atalay S (2017) Process Saf Environ Prot 111:270.
26. Zhu JN, Zhu XQ, Cheng FF, Li P, Wang F, Xiao YW, Xiong WW (2019) Appl Catal Environ 256B: 117830.
27. Zhou H, Kang L, Zhou M, Zhong Z, Xing W (2018) Chin J Chem Eng 26:1896.
28. Soltani T, Lee BK (2017) Chem Eng J 313:1258.
29. Pachamuthu MP, Karthikeyan S, Maheswari R, Lee AF, Ramanathan A (2017) Appl Surf Sci 393:67.
30. Lai C, Huang F, Zeng G, Huang D, Qin L, Cheng M, Zhang C, Li B, Yi H, Liu S, Li L, Chen, L (2019) Chemosphere 2:910.
31. Cui X, Li J, Ng DHL, Liu J, Liu Y, Yang W (2019) Carbon 158:738.
32. Wang Z, Lai C, Qin L, Fu Y, He J, Huang D, Li B, Zhang M, Liu S, Li L, Zhang W, Yi H, Liu X, Zhou, X. (2020) Chem Eng J 392:124851.
33. Li X, Tian Z, Liang K, Wang Y (2019) J Photochem Photobio Chem 37915A:79.
34. Ni Q, Ma J, Fan C, Kong Y, Peng M, Komarneni S (2018) Ceram Int 44:19474.
35. Cui L, Fanglong H,Guangming Z, Danlian H, Lei Q, Min C, Chen Z, Bisheng L, Huan Y, Shiyu L, Ling Li (2018) Chemosphere 224: 910.
36. Zhang X, Ma J, Fan C, Peng M, Komarneni S (2019) J Alloys Compds 785:343.
37. Zhao W, Wei Z, Zhang X, Ding M, Huang S (2019) Mater Res Bull 124:110749.
38. Qu J, Yu Z, Zang Y, Gu J, Jin J, Gao F (2019) New Carbon Mater 34:539.
39. He Y, Jiang DB, Jiang DY, Chen J, Zhang YX (2017) J Hazard Mater 344:230.
40. Zhao W, Wei Z, Zhang X, Ding M, Huang S, Yang S (2020) Appl Catal A Gen 5935:117443.
41. Wang A, Chen Z, Zheng Z, Xu H, Wang H, Hu K, Yan K (2020) Chem Eng J 379:122340.
42. Ling L, liu Y, Pan D, Lyu W, Xu X, Xiang X, Lyu M, Zhu, L (2019) Chem Eng J 381:122607.
43. Xia H, Zhang Z, Liu J, Deng Y, Zhang D, Du P, Zhang S, Lu, X (2019) Appl Catal Environ 259B:118058.
44. Li Y, Chen D, Fan S, Yang T (2018) J Taiwan Inst Chem E 9:185.
45. He F, Ji Y, Wang Y, Zhang Y (2017) J Taiwan Inst Chem E 80:553.
46. Wang A, Wang H, Deng H, Wang S, Shi W, Yi Z, Qiu R, Yan K (2019) Appl Catal Environ 248B:298.
47. Shoueir K, El-Sheshtawy H, Misbah M, El-Hosainy H, El-Mehasseb I, El-Kemary M (2018) Carbohydr Polym 197:17.
48. Chen Z, Zheng Y, Liu Y, Zhang W, Wang Y, Guo X, Tang X, Zhang Y, Wang Z, Zhang T (2019) Mater Chem Phys 238:121893.
49. Mahamallik P, Pal A (2017) J Environ Chem Eng 5:2886.
50. Hu X, Li R, Zhao S, Xing Y (2017) Appl Surf Sci 396:1393
51. Cheng M, Zeng G, Huang D, Lai C, Liu Y, Zhang C, Wan J, Hu L, Zhou C, Xiong W (2018) Water Res 138:7.
52. Han X, Chen T, Li J, Cheng F, Zhang M, Guo M (2020) J Photochem Photobio Chem 390A:112308.
53. Shao L, Gao J, Xia X, Dong W, Cheng S, Zhu Y, Liu Y (2019) J Photochem Photobio Chemistry 382A:111972.
54. Gong Q, Liu Y, Dang Z (2019) J Hazard Mater 371:677.
55. Wang Y, Xi Y, Tian H, Fang J, Quan X, Pei Y (2019) Catal Today 335:460.
56. Yu L, Chen J, Liang Z, Xu W, Chen L, Ye D (2016) Sep Purif Technol 171:80
57. Xie A, Cui J, Yang J, Chen Y, Lang J, Li C, Yan Y, Dai J (2019) Appl Catal Environ 264B:118548.
58. Li Q, Kong H, Li P, Shao J, He Y (2019) J Hazard Mater 373:437.
59. Jin H, Dong J (2019) Colloids Surf A 581:123803.
60. Su S, Liu Y, Liu X, Jin W, Zhao Y (2018) Chemosphere 218:83.
61. Li S, Zhang G, Zhang W, Zheng H, Zhu W, Sun N, Zheng Y, Wang P (2017) Chem Eng J 326:756.
62. Liu Y, Jin W, Zhao Y, Zhang G, Zhang W (2017) Appl Catal Environ 206B:642.
63. Xu HY, Li B, Shi TN, Wang Y, Komarneni S (2018) J Colloid Interface Sci 532:161.
64. Liu Y, Liu X, Zhao Y, Dionysiou DD (2017) Appl Catal Environ 213B:74.
65. Ma Y, Meng F, Wang Y, Lv X, Yang (2018) Appl Catal Gen 566A:60.
66. Nguyen LV, Busquets R, Ray S, Cundy AB (2017) Chem Eng J 307:159.
67. Zhu R, Zhu Y, Xian H, Yan L, Fu H, Zhu G, Xi Y, Zhu J, He H (2020) Appl Catal Environ 270B:118891.
68. Wei L, Zhang Y, Chen S, Zhu L, Liu X, Kong L, Wang L (2018) J Environ Sci 76:188.
69. Liu Y, Fan Q, Wang J (2018) J Hazard Mater 342:166.
70. Tekin G, Ersöz G, Atalay S (2018) J environ Chem Eng 6:1745.
71. Qian X, Ren M, Zhu Y, Yue D, Han Y, Jia J, Zhao Y (2017) Environ Sci Technol 51(7):3993.
72. Miao W, Ying Liu Y, Xiaoyan Chen X, Yixin Zhao Y, Shun Mao S (2020) Carbon 159:461.
73. Long Q, Liu F, Yuan Y, Dai Y, Wang C, Li X, Zhang J (2020) Colloids Surf A 594: 12465.
74. Espinosa JC, Catalá C, Navalón S, Ferrer B, Álvaro M, García H (2018) Appl Catal Environ 226B:242.
75. Wang K, Niu H, Chen J, Song J, Mao C, Zhang S, Gao Y (2017) Appl Surf Sci 404:138.
76. Zou C, Meng Z, Ji W, Liu S, Shen Z, Zhang Y, Jiang N (2018) Chinese J Catal 39:1051.
77. Saleh R, Taufik A (2018) Sep Purif Technol 210:563.
78. Yu Y, Huang F, He Y, Liu X, Song C, Xu Y, Zhang Y (2019) Sci Total Environ 654:942.
79. Yao T, Jia W, Feng Y, Zhang J, Lian Y, W J, Zhang X (2018) J Hazard Mater 362:62.
80. Wen H, Gu L, Yu H, Qiao X, Zhang D, Ye J (2018) Chem Eng J 352:837.
81. Li D, Yang T, Li Y, Liu Z, Jiao W (2019) J Clean Prod 246:119033.
82. Oruç Z, Ergüt M, Uzunoğlu D, Özer A (2019) J Environ Chem Eng 7:103231.
83. Guo X, Wang K, Li D, Qin J (2017) Appl Surf Sci 420:792.
84. Qian X, Wu Y, Kan M, Fang M, Yue D, Zeng J, Zhao Y (2018) Appl Catal Environ 237B:513.
85. Ye Y, Yang H, Wang X, Feng W (2018) Mat Sci Semicon Proc 82:14.
86. Bicalho HA, Lopez JL, Binatti I, Batista PFR, Ardisson JD, Resende RR, Lorençon E (2017) Mol Catal 435:156.
87. Sahar S, Zeb A, Liu Y, Ullah N, Xu A (2017) Chinese J Catal 38:2110.
88. He D, Chen Y, Situ Y, Zhong L, Huang H (2017) Appl Surf Sci 425:862.
89. Wang Q, Wang P, Xu P, Li Y, Duan J, Zhang G, Hu Li, Wang X, Zhang W (2020) Appl Catal Environmental 266B:118653.
90. Zhang J, Zhang G, Ji Q, Lan H, Qu J, Liu H (2020) Appl Catal Environmental 266B:118665.
91. Shao Y, Ruan J, Li X, Li Y, Chen H (2020) Process Saf Environ Prot 136:288.
92. Ma J, Jia N, Shen C, Liu W, Wen Y (2019) J Hazard Mater 378:120782.
93. An X, Wu S, Tang Q, Lan H, Tang Y, Liu H, Qu J (2018) Catal Commmun 112:63.
94. Ding Q, Lam FLY, Hu X (2019) J Environ Manage 244:23.
95. Hu J, Zhang P, An W, Liu L, Liang Y, Cui W (2018) Appl Catal Environ 245B:130.
96. Ma J, Yang Q, Wen Y, Liu W (2017) Appl Catal Environ 201B:232.
97. Niu H, He D, Yang Y, Lv H, Cai Y, Liang Y (2019) Appl Catal Environ 256B:117820.
98. Li X, Pi Y, Wu L, Xia Q, Wu J, Li Z, Xiao J (2017) Appl Catal Environ 202B: 653.
99. Wang Z, Lai C, Qin L, Fu Y, He J, Huang D, Li B, Zhang M, Liu S, Li L, Zhang W, Yi H, Liu X, Zhou X (2020) Chem Eng J 392:124851.
100. Fu H, Song XX, Wu L, Zhao C, Wang P, Wang CC (2020) Mater Res Bull 125:110806.
101. Ahmad M, Quan X, Chen S, Yu H (2020) Appl Catal Environ 264B:118534.
102. Ye Z, Padilla JA, Xuriguera E, Brillas E, Sirés I (2020) Appl Catal Environ 266B:118604.

103.Taha AA, Huang L, Ramakrishna S, Liu Y (2020) J water Process Eng 33:101004.
104.Ahmad M, Chen S, Ye F, Quan X, Afzal S, Yu H, Zhao X (2018) Appl Catal Environ 245B:428.
105.Wu Q, Yang H, Kang L, Gao Z, Ren F (2019) Appl Catal Environ 263B:118282.
106.Gao C, Chen S, Quan X, Yu H, Zhang Y (2017) J Catal 356:125.
107.MacDonald MJ, Cho DW, Yu IKM, Tsang DCW, Yip ACK (2018) Sci Total Environ 644:389.
108.Tang J, Wang J (2018) Chem Eng J 351:1085.
109.Martínez F, Leo P, Orcajo G, Díaz-García M, Sanchez-Sanchez M, Calleja G (2018) Catal Today 313:6.
110.Mei W, Song H, Tian Z, Zuo S, Li D, Xu H, Xia D (2019) Mater Res Bull 119:110570.
111.Nguyen VH, Bach LG, Bui PQT, Nguyen TD, Vo DVN, Vu HT, Do ST (2018) J Environ Chem Eng 6:7434.
112.Cao P, Quan X, Zhao K, Chen S, Yu H, Niu J (2019) J Hazard Mater 382:121102.
113.Cheng M, Lai C, Liu Y, Zeng G, Huang D, Zhang C, Qin L, Hu L, Zhou C, Xiong W (2018) Coord Chem Rev 368:80.
114.Wang N, Du Y, Ma W, Xu P, Han X (2017) App Catal Environ 210B:23.
115.Pan Y, Jiang S, Xiong W, Liu D, Li M, He B, Fan X, Luo, D. (2019) Microporous Mesoporous Mater 291:109703
116.Huang X, Zhu N, Mao F, Ding Y, Zhang S, Liu H, Li F, Wu P, Dang Z, Ke Y (2019) Chem Eng J 392:123636.
117.Gogoi A, Navgire M, Sarma KC, Gogoi P (2017) Chem Eng J 311:153.
118.Ouyang J, Zhao Z, Suib SL, Yang H (2018) J Colloid Interface Sci 539:13.
119.Eshaq G, Wang S, Sun H, Sillanpaa M (2019) J Hazard Mater 382:121059.
120.Tap Van H, Huong Nguyen L, Kien Hoang T, Pha Tran T, Tuan Vo A, Pham TT, Nguyen XC (2019) Sep Purif Technol 224: 431.
121.Qu J, Che T, Shi L, Lu Q, Qi S (2019) Chin Chem Lett 30:1198.
122.Du D, Shi W, Wang L, Zhang J (2017) Appl Catal Environ 200B:484.
123.Cohen M, Ferroudj N, Combes A, Pichon V, Abramson S (2019) J Environ Chem Eng 7:102987.
124.Zhou L, Lei J, Wang L, Liu Y, Zhang J (2018) Appl Catal Environ 237B:1160.
125.Vasilyeva MS, Rudnev VS, Zvereva AA, Ustinov AY, Arefieva OD, Kuryavyi VG, Zverev GA (2018) J Photochem Photobio Chem 356A:38.
126.Meng Q, Wang K, Tang Y, Zhao K, Zhang G, Zhao L (2017) J Alloys Compds 722:8.
127.Uma K, Arjun N, Pan GT, Yang TCK (2017) Appl Surf Sci 425:377.
128.Liu X, Sun C, Chen L, Yang H, Ming Z, Bai Y, Feng S, Yang ST (2018) Mater Chem Phys 213:231.
129.Jia Z, Kang J, Zhang WC, Wang WM, Yang C, Sun H, Habibia D, Zhang, LC (2017) Appl Catal Environ 204B:537.